Source Separation From Single-Channel Recordings by Combining Empirical-Mode Decomposition and Independent Component Analysis

Bogdan Mijović*, *Student Member, IEEE*, Maarten De Vos, *Member, IEEE*, Ivan Gligorijević, Joachim Taelman, *Member, IEEE*, and Sabine Van Huffel, *Fellow, IEEE*

***Abstract*—In biomedical signal processing, it is often the case that many sources are mixed into the measured signal. The goal is usually to analyze one or several of them separately. In the case of multichannel measurements, several blind source separation techniques are available for decomposing the signal into its components [e.g., independent component analysis (ICA)]. However, only a few techniques have been reported for analyses of single-channel recordings. Examples are single-channel ICA (SCICA) and wavelet-ICA (WICA), which all have certain limitations. In this paper, we propose a new method for a single-channel signal decomposition. This method combines empirical-mode decomposition with ICA. We compare the separation performance of our algorithm with SCICA and WICA through simulations, and we show that our method outperforms the other two, especially for high noise-to-signal ratios. The performance of the new algorithm was also demonstrated in two real-life applications.**

***Index Terms*—Blind source separation (BSS), empirical-mode decomposition (EMD), feature extraction, independent component analysis (ICA), single-channel signal analysis.**

I. Introduction

In THE field of biomedical signals, independent sources are often mixed together in the measured signal. Our task is then to unmix contribution sources in order to have a closer look at the signal of interest. In multichannel recordings, such as EEG, this problem is efficiently handled by employing *blind source separation* (BSS) techniques to unmix the given signal into sources (see, e.g. [1]–[3]).

Manuscript received November 18, 2009; revised April 9, 2010; accepted April 30, 2010. Date of publication June 10, 2010; date of current version August 18, 2010. This work was supported by the Research Council, Katholieke Universiteit Leuven under Project GOA-AMBioRICS, Project GOA MaNet, Project CoE EF/05/006, and Project IDO 05/010 EEG-fMRI, by the the Flemish Government Ph.D./Postdoctoral Grants under Project FWO: G.0427.10N (Integrated EEG–fMRI), Project IWT: TBM070713-Accelero, and Project TBM080658-MRI (EEG–fMRI), by the Belgian Federal Science Policy Office IUAP P6/04 (Dynamical systems, control, and optimization), and by the European Union under NeuroMath (European Cooperation in Science and Technology BM0601). *Asterisk indicates corresponding author*.

*B. Mijović is with the Department of Electrical Engineering, SISTA-COSIC-DOCARCH Division, Katholieke Universiteit Leuven, Leuven 3001, Belgium (e-mail: bogdan.mijovic@esat.kuleuven.be).

M. De Vos, I. Gligorijević, J. Taelman, and S. Van Huffel are with the Department of Electrical Engineering, SISTA-COSIC-DOCARCH Division, Katholieke Universiteit Leuven, Leuven 3001, Belgium.

Color versions of one or more of the figures in this paper are available online at http://ieeexplore.ieee.org.

Digital Object Identifier 10.1109/TBME.2010.2051440

Independent component analysis (ICA) is a BSS technique that extracts statistically independent sources [called independent components (ICs)] from a set of recorded signals. Standard algorithms tackle the problem when the number of electrodes (channels) is larger than or equal to the number of sources. On the other hand, there is a group of algorithms called "undetermined ICA," which can recover more signals than channels available (see, e.g. [4], and references herein). In the limit, the goal can be the extraction of independent sources from a single-channel recording, for example, cleaning the electromyogram (EMG) signal contaminated by an ECG artifact [5], [6], especially from the electrodes placed on the left side of the back. The ECG artifact is very prominent in this case. Another example is in single-channel deep brain recordings, where the neuronal-spikes are very high noise-to-signal ratio (NSR) signals and are not easy to separate from noise [7], [8]. It could also be useful in preprocessing when applied to the multichannel signals (cleaning the eye artifacts from the EEG signal, extraction of event-related potentials (ERP) etc.).

The adaptation of ICA to single-channel signals, called single-channel ICA (SCICA), has already been proposed in [9]. It has two major drawbacks: first, the algorithm assumes stationary sources, and second, the sources are assumed to be disjoint in the frequency domain. These assumptions, however do not always hold in applications.

Another approach of decomposing a signal of interest into different sources is as follows. If a multichannel recording can be created from a single-channel signal, ICA might be used to select the signal components, which are independent from each other. One way to decompose a single-channel signal into multiple components is to decompose it into different spectral modes (e.g., using a wavelet transform or empirical-mode decomposition (EMD) [10]).

A wavelet decomposition splits up a signal at each step in a predetermined manner by means of predefined linear time-invariant filters, thereby precluding the possibility of adapting the decomposition to local variations of the oscillation. The wavelet-ICA (WICA) technique has been proposed in [11]. A wavelet transform is used to expand a 1-D signal into 2-D by dividing it into its frequency subbands. Then, ICA is used to extract the sources. However, in the field of biomedical signal processing, it has always been referred to as a multichannel signal-processing technique, where the wavelet transform has been used only for denoising (e.g., for extracting ECG artifacts from the EMG signal, when the latter has also been recorded in

0018-9294/$26.00 © 2010 IEEE

parallel [12], or for separating the fetal ECG from mother ECG when six ECG signals were recorded in parallel [13]).

The EMD is a signal-analysis tool that is able to decompose any time series into a set of spectrally independent oscillatory modes, called intrinsic-mode functions (IMFs). The advantage of EMD, compared to wavelets, is that the EMD is a data-driven algorithm. This means that it decomposes a signal in a natural way without prior knowledge about the signal of interest embedded in the data series [14].

Here, we propose a new technique for single-channel signal analysis, which first decomposes the given signal into *spectrally independent* modes using EMD algorithm, and then, ICA is applied to extract *statistically independent sources*. At the time of writing this paper, we discovered another abstract [15], including figures, mentioning a similar idea. However, no simulation or comparison study has been provided. Also, contrary to the mentioned work, no IMF subset is preselected here before applying the ICA technique.

In this paper, we introduce the new algorithm combining EMD and ICA and study its source-extraction capabilities in depth in single-channel signal processing. In particular, we compare our algorithm to WICA and SCICA by means of an extensive simulation study. Additionally, we show the performance of the algorithm in two real-life applications.

The paper is organized as follows. In Section II, all the methods and algorithms used in this paper are shortly described. Next, in Section III, we compare the performance of the described methods in a simulation setup. We will show the performance of the methods applied to two real-life examples in Section IV. In addition, we provide in-depth study of the possibilities and advantages of this technique, as well as its drawbacks and limitations. A short conclusion summarizes the main ideas.

II. Methods

In this section, we first revise some existing methods SCICA and WICA in Section II-B and C, and then, we describe the new method ensemble EMD–ICA (EEMD–ICA) in Section II-D.

A. Independent Component Analysis

As ICA is a building block in all the other algorithms, we start with a short description. The goal of ICA is to separate instantaneously mixed signals from the channel matrix $\mathbf{X}$ into their independent sources $\mathbf{S}$, such that $\mathbf{X} = \mathbf{MS}$, where $\mathbf{M}$ is called the mixing matrix, without prior knowledge. It is possible to estimate the contributing sources from the mixtures provided; they are statistically independent of each other. There are several ways to solve this problem. Here, we used the popular FastICA algorithm [16], [17]. It is based on a fixed-point iteration scheme for finding a maximum of the non-Gaussianity of the sources. It is to be noted that this algorithm performs best if the distribution of the sources is "*generalized normal distribution*" $\left(p(x) = C \times e^{-\alpha|x|^{\gamma}}, \gamma \neq 2\right)$ [18]. In this formula, $\gamma = 2$ gives Gaussian distribution.

Algorithm 1 SCICA

1. First break up a time series $x(t)$ into a sequence of contiguous blocks $\mathbf{x}(k)$
2. Apply the FastICA algorithm to this matrix, to derive the unmixing matrix $\mathbf{W}$
3. Extract the particular source of interest simply by filtering the original signal $x(t)$ with the corresponding row of the matrix $\mathbf{W}$.
4. To obtain the appearance of the desired source in the signal $x(t)$, multiply the extracted source $s(i)$ with the i-th column of the matrix $\mathbf{M}$.
5. Now subtract the appearance of the source $s(i)$ in the signal x, redefine this newly obtained signal as $x(t)$, and repeat the steps from 1 to 4 to further extract other sources from the new signal x obtained after this subtraction.

B. Single-Channel ICA

SCICA is an adaptation of the ICA algorithm to single-channel signals [9]. The algorithm is explained as follows.

First, the signal $x(t)$ is broken up into a the sequence of contiguous blocks $\mathbf{x}$, each having length N, which is to be treated as a sequence of vector observations. Then, the matrix $\mathbf{X}$ is formed as a set of observations $\mathbf{x}(k)$, $k = 1, 2, \ldots, K$, as follows:

$$\mathbf{x}(k) = [x(k\tau), \ldots, x(k\tau + N - 1)]^T$$
$$\mathbf{X} = [\mathbf{x}(1), \ldots, \mathbf{x}(K)]^T \quad (1)$$

where k is the block index, τ is a time delay, and $(K\tau + N - 1)$ is the length of the original signal. Note that the performance of SCICA algorithm significantly depends on these parameters. However, in the paper where the algorithm is originally introduced [9], Davies and James leave to readers to set fix these parameters based on their own experience. Every row in the matrix $\mathbf{X}$ corresponds now to a single observation. Then, we apply the FastICA algorithm to the matrix $\mathbf{X}$ to derive the mixing and unmixing matrix $\mathbf{M}$ and $\mathbf{W}$. Now, the matrix $\mathbf{W}$ yields the inverse filters we were looking for in its rows, and extracting the particular source of interest is achieved by simply filtering the signal $x(t)$ with the corresponding row of the matrix $\mathbf{W}$.

FastICA provides the mixing matrix $\mathbf{M}$ (which is actually the matrix of filters) as an inverse (or the pseudoinverse if the number of sources and the number of channels differ) of $\mathbf{W}$ $\left(\mathbf{M} = \mathbf{W}^{-1}\right)$. Therefore, we can simply multiply the extracted source $S(i)$ with the ith column of the matrix $\mathbf{M}$ to obtain its appearance in the original signal. When we subtract the first-derived source from the original signal, we can extract the second one form this deflated signal and so on.

This algorithm assumes that the signal is stationary and it is composed of spectrally nonoverlapping sources. In this case, filters can be derived with passbands that correspond to frequency bands of these sources. SCICA estimates these filters and convolves the signal to extract the sources one by one. The algorithm is therefore blind deconvolution, rather than BSS technique. It is shortly outlined in Algorithm 1 and discussed in detail in [9].

Algorithm 2 Wavelets-ICA (WICA)

1. Select the mother wavelet and the order of the Wavelet transform.
2. Apply the Wavelet decomposition to generate the input matrix for the ICA algorithm
3. Perform the FastICA algorithm to the set of wavelet components and derive the corresponding mixing and unmixing matrices $\mathbf{M}$ and $\mathbf{W}$
4. Select the source(s) of interest and multiply it with mixing matrix $\mathbf{M}$ to back-reconstruct its appearance in the set of wavelet components
5. Sum over all the rows of this matrix to back-reconstruct the appearance of the particular source in the original signal

Algorithm 3 EEMD-ICA

1. Add independent, identically distributed white noise with zero-mean and SD equal to np times the SD of the original signal.
2. Apply EMD to derive a set of IMFs.
3. Repeat steps 1 and 2 a number of times, resulting into an ensemble of IMF sets.
4. Average over the ensemble to obtain a set of averaged IMFs
5. Perform the FastICA algorithm to the IMFs and derive the corresponding mixing and unmixing matrices $\mathbf{M}$ and $\mathbf{W}$
6. Select the independent component (source) of interest and multiply it with mixing matrix $\mathbf{M}$ to back-reconstruct its appearance in the IMF set
7. Sum over all the newly derived IMFs to reconstruct the appearance of the source of interest in the original signal

C. Wavelet-ICA

Since the wavelet analysis is based on very similar ideas as the EMD, i.e., to decompose the signal into components of disjoint spectra, it was natural to compare the performance of the EEMD–ICA algorithm with the WICA algorithm. First, we have to choose the mother wavelet. The best way of choosing it is that it corresponds in shape with the source we were interested in. Note that with no *a priori* knowledge of the signal of interest, it is very hard to make this decision.

After choosing the appropriate mother wavelet, also the order of the wavelet transform has to be chosen. Then, the signal is decomposed into spectrally nonoverlapping components using a wavelet decomposition. The ICA algorithm is then applied to the derived components. The ICA algorithm provides us with mixing and unmixing matrices $\mathbf{M}$ and $\mathbf{W}$, and a matrix of ICs $\mathbf{S}$ as an output, where the matrix of wavelet components ($\mathbf{X}$) satisfies the equation $\mathbf{X} = \mathbf{MS}$, and $\mathbf{S} = \mathbf{WX}$. Note that the interpretation of the mixing matrix $\mathbf{M}$ is different here. It does not mix sources into different channels, but into the set of wavelet components instead. After selecting the sources of interest (this part has to be done manually or by exploiting *a priori* knowledge about the source of interest), the appearance of the particular source in the signal is achieved by multiplying that source with the mixing matrix $\mathbf{M}$ (to derive its appearance in the wavelet components), and consequently, summing over all the newly derived wavelet components. Contrary to the SCICA algorithm, this algorithm makes no assumption on spectral characteristics of the sources. Assumptions about the statistical properties depend on the ICA algorithm used in the second step of the method. The algorithm is described in Algorithm 2.

D. Ensemble EMD–ICA (EEMD–ICA)

EMD is a single-channel technique [10] that decomposes any complicated time series into a finite set of *oscillatory modes* called IMFs. IMFs are meant to be *monocomponent*, zero-mean oscillatory functions, which are orthogonal to each other and a set of IMF's should be complete. Here, the term monocomponent means that all the IMF's contain only one frequency at the time, which is called the instantaneous frequency. The orthogonality property implies that different IMF's do not have similar frequency content. Oscillatory here means that they have the same number of local maxima and minima, and all the maxima are positive, and the minima are negative.

One of the major drawbacks of the original EMD algorithm is that it is highly sensitive to noise. Therefore, a more robust, noise-assisted version of the EMD algorithm, called EEMD, was introduced [19]. The algorithm defines the IMF set for an ensemble of trials, each one obtained by applying EMD to the signal of interest with added independent, identically distributed white noise of the same standard deviation (SD). Taking into account properties of the white noise, noisy components are expected to be canceled out. The ratio of the noise SD to the SD of the signal will further be referred to as a *noise parameter* (np). The EEMD algorithm is available online in [20].

After EEMD is performed and a set of averaged IMFs is derived (last IMF being only the monotonic function with at most one extremum), FastICA is applied to the whole set of IMFs. The IC's are extracted as well as the mixing and demixing matrices, $\mathbf{M}$ and $\mathbf{W}$, as described in Section II-C. After selecting the ICs of interest, the signal is reconstructed first by multiplying it by the mixing matrix to derive a new IMF set, in which only the IC of interest is present. Summing over the newly derived IMF set, similarly as shown in Section II-C, the appearance of the desired source in the original signal is obtained.

It is worth noting that, contrary to the work of Xing and Hou [15], no IMF subset has been preselected as an input of the ICA algorithm in order to keep this part of the algorithm as automatic as possible. We afterward select the IC we are interested in. Note that this part has to be done by visual inspection, unless some features of the signal of interest are known. The reconstruction of the signal is then straightforward. We multiply the IC vector with the mixing matrix to regenerate the IMF set, now containing only the component of interest, and then, simply add all of these IMFs together to obtain the reconstructed signal. This algorithm, as well as WICA makes no assumption on spectral characteristics of the sources. Statistical properties of the sources depend on the ICA algorithm used (see Algorithm 3).

III. SIMULATIONS

To evaluate the performance of the EEMD–ICA method in biomedical single-channel signal processing and to compare its performance in an objective way with the other available methods, as outlined in Section II (WICA and SCICA), we performed the following two essentially different simulations. In Section III-A1, the signal of interest we aim to extract is a stationary signal of oscillatory type. As an example, we chose the extraction of a seizure event from a real-life background EEG signal contaminated by muscle artifact. In this case, the signal of interest is a stationary signal of oscillatory type that is representative for different physiological signals, such as blood pressure, respiration, EEG α-rhythm, even heart rate series in some cases, etc. In the second simulation, as described in Section III-A2, the signal of interest we want to extract is spiky. As an example, we focus on the extraction of an ECG artifact from a real-life EMG signal. Simply subtracting it from the original signal cleans up the EMG data. This spiky type of data are representative for a whole class of artifact-removal problems, such as extraction of the ECG artifact from other physiological signals like EEG, the extraction of interictal spikes in EEG signals, spiky-type seizure detection in neonatal EEG [21], as well as spike detection in intracranial electroneural signals captured during deep brain recordings [7].

In the simulations, we always mixed two signals: the signal we want to extract ($a(t)$), and another, unwanted signal, which is considered to be noise ($b(t)$) in the following way:

$$x_\lambda(t) = a(t) + \lambda b(t) \tag{2}$$

with $\lambda \in \mathbb{R}$ being a proportion factor, and $x_\lambda(t)$ being a mixed signal, i.e., an input to the algorithm. An important measure here is the NSR, which is defined as follows:

$$\text{NSR} = \frac{\text{RMS}(\lambda b(t))}{\text{RMS}(a(t))}. \tag{3}$$

Changing λ alters the NSR of our simulated signals. The NSR measure is used here rather than the more common SNR to equally emphasize the behavior of the signal in the range of NSR from 0.05 to 1 (the power of noise is 5% to 100% of the signal power), and the range of NSR from 1 to 2 (100% to 200%). Note that NSR is simply the inverse of SNR.

The simulation performance is expressed in terms of the relative root mean squared error (RRMSE) as follows:

$$\text{RRMSE} = \frac{\text{RMS}(a(t) - \hat{a}(t))}{\text{RMS}(a(t))} 100\,[\%] \tag{4}$$

where $\hat{a}(t)$ is the estimate of the signal of interest.

A. Simulations Setup

1) Extraction of an Oscillation-Type Source: To simulate the extraction of oscillation-type components, we consider here the extraction of a seizure event from single-channel brain recordings. The brain signal consists of awake background electrical activity from a normal subject contaminated by muscle artifact. The simulated muscle artifact was superimposed on real-life brain background activity. This defines the noise part $b(t)$ in this simulation. The amplitude of the muscle artifact was chosen in a realistic way. Epileptic activity can be modeled in two ways—either as spiky activity, or as a pure sinusoid. Here, the epileptic activity was modeled as a 4-Hz sinusoidal waveform. The frequency of the background electrical activity ranges from 0 to 30 Hz, so the spectra of the sinusoid and the background activity were overlapping. The sinusoidal signal in these simulations is denoted as $a(t)$. Signals $a(t)$ and $b(t)$, as well as the mixed signals for different NSR's are shown in Fig. 1.

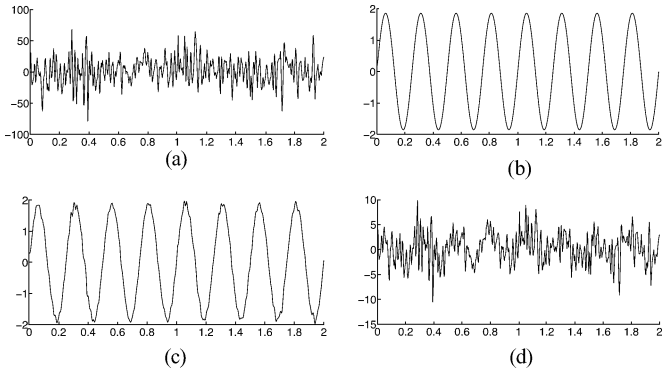


Fig. 1. (a) Simulated background brain signal with the muscle artifact—signal $b(t)$. (b) Sinusoidal signal—$a(t)$. (c) Signal $x(t)$ for NSR $= 0.05$. (d) Signal $x(t)$ for NSR $= 2$.

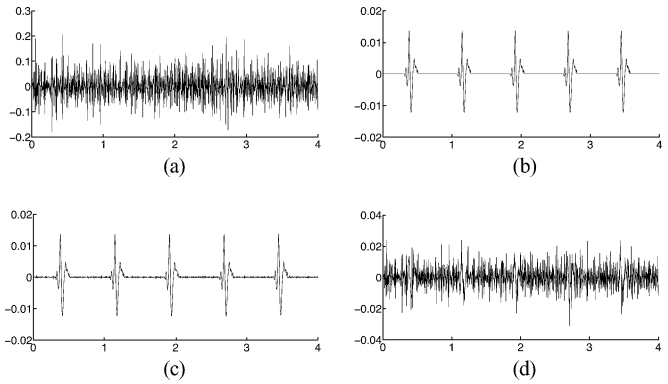


Fig. 2. (a) Pure EMG—signal $b(t)$. (b) Spike train—signal $a(t)$. (c) $x(t)$ for NSR $= 0.05$, (d) $x(t)$ for NSR $= 2$.

2) Extraction of a Spike-Type Source: To simulate the extraction of spiky-type sources, we mixed a pure real-life EMG signal (signal $b(t)$) with a simulated ECG artifact—a spike train (signal $a(t)$) for different NSR values, as described earlier. The spike-train signal was a real-life QRS complex recorded from the EMG electrode repeated every 0.75 s, and zero padded in between. The mentioned single spike is extracted from the EMG electrode, while no muscle activity was present. These signals are shown in Fig. 2. The frequency spectrum of the EMG signal is broadband (10–180 Hz) with more or less equally distributed power over the whole range, while the spike train is a narrowband signal (5–30 Hz). Note that the spectra of these two signals are also overlapping.

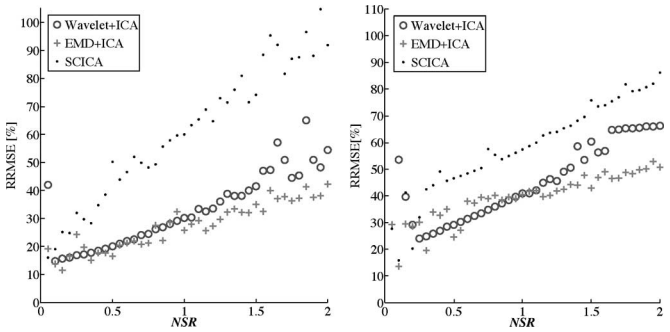


Fig. 3. Comparison of algorithms performances for the simulation described in (left) Section III-A1 and (right) III-A2.

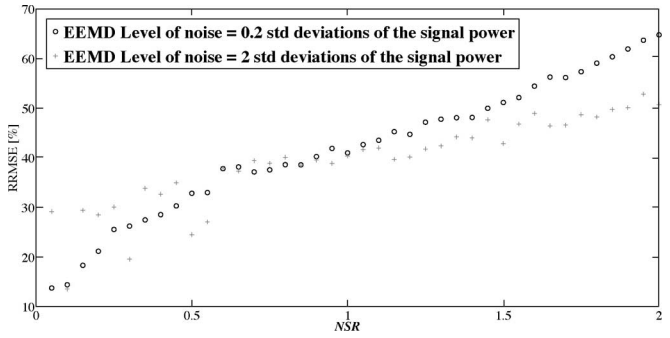


Fig. 4. Comparison of the EEMD–ICA algorithm for different levels of added noise for spike-type simulation.

B. Parameter Settings

In all the simulations, the number of ICs in FastICA to be extracted was set to 5 in Section III. In the SCICA algorithm, the values for K and τ were set to 10 and 1, respectively (these values yielded the best performance in terms of RMSE). The mother wavelet used in the WICA algorithm was Daubechies 6, and the order of the wavelet transform was set to 8. In the EEMD–ICA simulations, the np-value used was set to 2. The number of IMF's was usually observed to be between 8 and 15 components, and it only depends on the complexity of the signal (if the signal is only the sinusoid, then the number of IMFs will theoretically be 1 and the residue, which is the mean value). Also, the NSR was set to increase from 0.05 to 2 with steps of 0.05.

C. Simulation Results

Fig. 3 shows the performance of all the algorithms outlined in Section II as a function of NSR for the simulations in Section III-A1 and III-A2, respectively. Additionally, Fig. 4 compares the performance of the EEMD–ICA algorithm for two different np values (0.2 and 2), as this is a crucial parameter.

Figs. 5 and 6 illustrate the EEMD decompositions of the mixed signal from the simulation given in Section III-A1 and III-A2, respectively, for the NSR $= 1$ before applying the ICA algorithm. The first row shows the original signal, and the other rows show different IMFs. Figs. 7 and 8 show the extracted ICs after applying FastICA and signal reconstruction. In both simulations, the signal of interest is nicely captured in the first component.

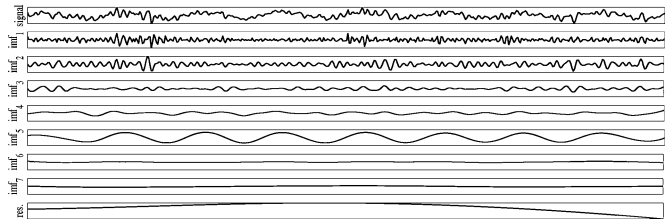


Fig. 5. EEMD decomposition of the signal composed of background EEG, muscle artifact, sinusoidal seizure, and noise for NSR $= 1$.

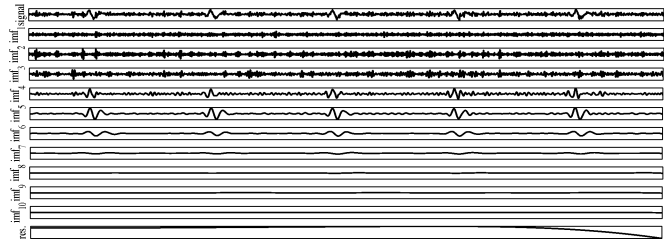


Fig. 6. EEMD decomposition of the EMG signal with ECG artifact (NSR $= 1$).

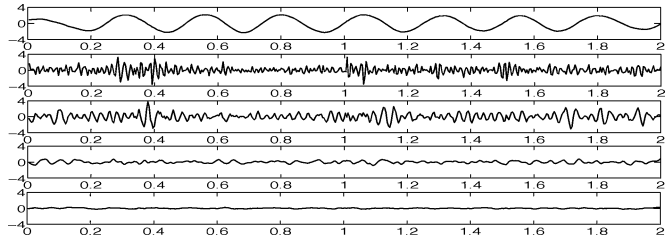


Fig. 7. Sources extracted with the EEMD-ICA decomposition of the signal from simulation 1 for NSR $= 1$.

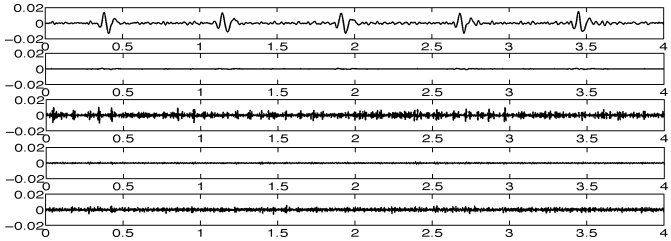


Fig. 8. Sources extracted with the EEMD-ICA decomposition of the signal from simulation 2 for NSR $= 1$.

In Figs. 9 and 10, the result of applying WICA is shown for oscillatory- and spike-type signal extraction simulations, respectively.

D. Simulation Discussion

Compared to other algorithms in our simulations, EEMD–ICA performs best for high NSR. For low NSR, EEMD–ICA performs similarly to WICA, although the tuning of the np may significantly increase the accuracy of the results. This is because too much noise is added for making an ensemble ($np = 2$), and the noise could not be canceled out correctly. From Fig. 4, it

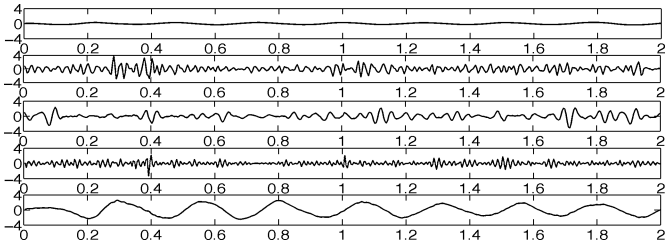


Fig. 9. Sources extracted with the WICA decomposition of the signal from simulation 1 for NSR $= 1$.

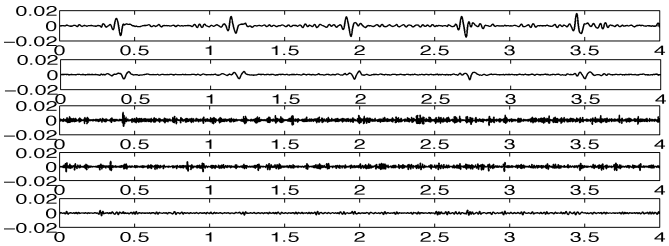


Fig. 10. Sources extracted with the WICA decomposition of the signal from simulation 2 for NSR $= 1$.

is clear that the algorithm's performance depends on this factor and performance for low NSR's can be significantly enhanced by reducing *np*. This is also one of the drawbacks of the EEMD–ICA algorithm in the sense that this parameter has to be chosen correctly in order to achieve the best performance; although, the inexperienced user can choose any value between 0 (the regular EMD) and 2 and obtain a satisfactory result. One way to choose the np is to set it to be equal to the NSR of the signal itself. If no knowledge of the noise power is present, either the regular EMD technique might be used, or several np values could be tried out, until the best separation is achieved. In [19], it is also shown that the np should be smaller if the signal we want to extract has high-frequency behavior and larger if the signal we want to extract is of low-frequency content.

The SCICA algorithm performed clearly worse than other algorithms in both simulations. The problem with this approach is that it yields two major limitations: First, the algorithm assumes stationarity of the data, and second, it is not able to separate components with overlapping spectra. In the first simulation (see Section III-A1), SCICA underperformed due to significant spectral overlapping of the data, although the signals to be extracted were stationary. In the second simulation (see Section III-A2), its performance was more comparable to that of the other algorithms, although it was inferior to that of the EEMD–ICA algorithm due to the nonstationarity and spectral overlapping of the data from the simulation.

It is worth noting that in the second simulation (see Section III-A2), the modeled ECG artifact was always spread over a number of ICs for the examples under study in WICA simulations (see Fig. 10), contrary to EEMD–ICA that could capture the signal of interest into one component only (see Fig. 8). It is also obvious that in the first simulation (see Section III-A1), the sinusoidal signal extracted with the EEMD–ICA algorithm (as illustrated in Fig. 7) was much smoother than the one extracted with WICA (see Fig. 9), despite the fact that the RRMSE in the simulation was almost equal for the particular case (NSR $= 1$). However, the WICA algorithm seemed to outperform a little bit the EEMD–ICA in the spiky-type source-extraction simulation in the low NSR range. Therefore, we show in Fig. 4, that by tuning the np parameter, the performance of EEMD–ICA can be significantly increased in this range. This tuning will weaken the performance for high NSR, although it will be still better than the one of WICA (RRMSE $= 50.73$ for $np = 2$ and RRMSE $= 64.79$ for $np = 0.2$ for EEMD–ICA, and RRMSE $= 66.22$ for WICA, see Fig. 4). Both the shape and the amplitude of the ECG artifact peak in the EMG simulation were almost perfectly recovered using the EEMD–ICA algorithm, contrary to the other methods, where the extracted spikes were mostly changed both in shape and amplitude.

The advantage of EEMD over wavelets is that EEMD breaks the signal into its oscillatory modes, and therefore, we expect the EEMD–ICA algorithm to outperform WICA in the case of oscillatory signals, which are very common in the field of biomedical data. Additionally, EEMD has a data-driven, instead of a predefined basis, contrary to wavelets and is able to deal with very local variations in the signal oscillations.

Since the spike-type data are not localized in frequency (simulation in Section III-A1, Fig. 6), EEMD will yield local oscillations in several IMFs. The latter ICA processing will capture these oscillations in only one IC. Here, the reader might argue that there is no obvious reason that variations in different IMFs are mutually dependent and independent from the rest of the signal.

To address this question, we refer to the work of Daubechies *et al.* [18], where they consider the use of the ICA algorithms Infomax [22] and FastICA on the blood-oxygen-level-dependent (BOLD) signal in functional MRI (fMRI) data. These algorithms are the two most widely used ICA algorithms to analyze fMRI data, although other more general ICA algorithms exist that assume less about components in the sense of their probability distribution function, like joint approximate diagonalization of eigen matrices (JADE) [23], and can separate mixtures into ICs for which FastICA and Infomax fail (FastICA and Infomax work well if the sources have "*generalized normal distribution,*" excluding Gaussian distribution). However, Infomax and FastICA showed to outperform JADE when separating the biological signals coming from different physiological sources, which do not have statistically independent distributions *per se*. The issue is that the variations in BOLD signal in different brain areas have no physiological reason to be statistically independent. Daubechies *et al.* show that the superior performance of Infomax and FastICA in fMRI is linked to their ability to effectively handle sparse components rather than ICs as such. Therefore, we also expect FastICA performed after the EEMD to pick up local oscillations from different IMFs, caused by spike appearance in the decomposed signal, and to capture them in only one IC.

When it comes to the oscillatory signals, it is obvious that the EEMD algorithm is able to extract the pure sinusoid itself (simulation in Section III-A1, Fig. 5), and therefore, EEMD-ICA will always give a good result in extracting the oscillatory

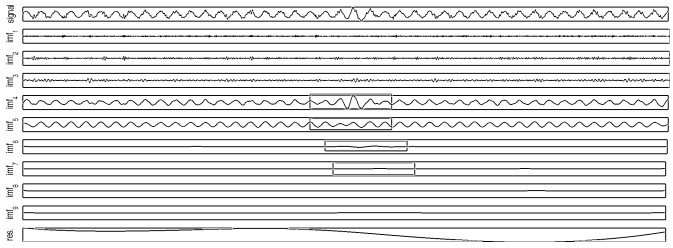


Fig. 11. EEMD of the single spike mixed with the sinusoid and the background EEG signal.

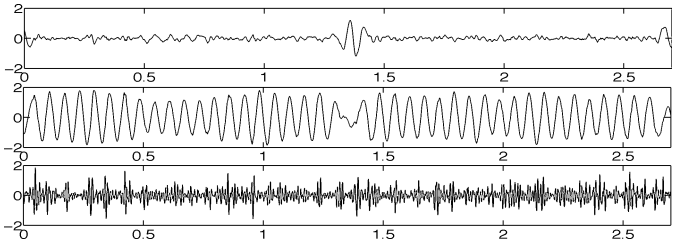


Fig. 12. EEMD–ICA decomposition of the single spike mixed with the sinusoid and the background EEG signal.

data. It is also clear that the postprocessing based on ICA might not improve the result, but the oscillatory signal is still nicely preserved, as apparent from Fig. 8. The question arises then: Why do we need the ICA step?

To answer this question, we will provide an additional simulation where we want to separate a single spike from a sinusoid and noise. In this simulation, we mixed three signals: the single spike in the middle of the signal, with the sinusoid and the background EEG activity from simulation given in Section III-A1.

The first row in Fig. 11 shows the original signal, where the spike is poorly (almost not) visible, and the other rows present the extracted IMFs. It is important to note that the EEMD was not able to separate the spike from the sinusoid-like seizure and the sinusoid is present in two IMF channels. It is evident that no simple arithmetical operation can be applied to IMFs to separate the spike from the sinusoid. However, if we apply FastICA (see Fig. 12), the spike is isolated in one channel, the sinusoidal seizure in another one, and the background EEG in the third channel. The sinusoid is apparently not perfectly recovered and is still distorted in the time instant of the spike appearance, due to the fact that the chosen spike had similar width as the period of the sinusoid. However, making use of this decomposition would allow spike-type or oscillatory-type seizure detection algorithms to perform significantly better.

We would like to stress here that applying the ICA technique on the IMF set makes sense only if the original sources and the IMFs are mutually linearly dependent, i.e., that the set of IMFs and the set of ICs span the same row space, which is not easy to prove. Furthermore, the EEMD itself is mathematically not well established, although it gives nice results in practical applications. Our simulations show, however, that combining EEMD and ICA clearly enhances source separation, and this will

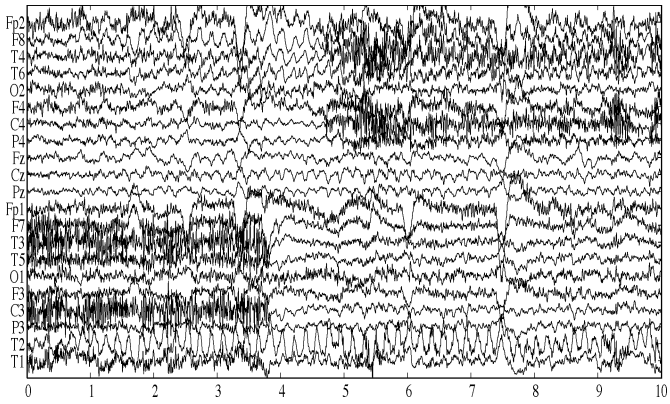


Fig. 13. Ten seconds of 21-channel EEG recordings.

be further illustrated in some real-life examples in the following sections.

IV. Real-Life Application of EEMD–ICA

To illustrate the performance of the proposed EEMD–ICA algorithm on two real-life applications, we consider two different cases. In the first case, we apply the EEMD–ICA algorithm to one of the EEG channels contaminated by muscle artifact, eye artifact, and seizure activity. We try to separate this information into different sources. In the second case, we will demonstrate how our new method performs in the case separating the ECG artifact from the EMG recordings, this time *in vivo*. In the EEMD–ICA algorithm, the number of ICs to be extracted was set to seven in the example given in Section IV-A1 because we were interested in three different sources and not all of them would appear in the first five IC's. In the example given in Section IV-A2, the number of IC's to be extracted was set to five.

A. Real-Life Examples

1) EEG Recordings: In Fig. 13, 10 s of 21-channel scalp EEG recordings from a long-term epilepsy monitoring unit are shown. This recording contains ictal activity from a patient with *mesial temporal lobe epilepsy* (MTLE), contaminated with eye blinks and muscle artifact. The sampling rate was 250 Hz. Although the single-channel technique in this case is not necessary, we chose this example because lower spatial sampling can be required in wireless systems applications, and our technique might be of use. Also, it enables us to further validate our technique. Eye artifacts can be observed around 2.5, 3.5, 6, and 7.5 s and are most emphasized in the Fp1 and Fp2 channels, as expected. Seizure activity is constantly present (T2 channel), and muscle activity starts on one side of the head. We will extract all underlying signals from channel T1 by applying EEMD–ICA, because their contributions are rather weak in this channel, and therefore, a successful extraction of these sources is most challenging.

2) EMG Recording: In the upper trace of Fig. 16, we give a recording of 100 s of the EMG signal contaminated with the ECG artifact. This recording corresponds to the phase

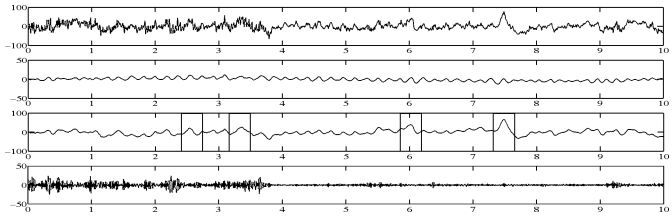


Fig. 14. Twenty-first EEG channel decomposed in the ICs. First row—original channel, second row—seizure event, third row—eye artifact (rectangles), and fourth row—muscle activity.

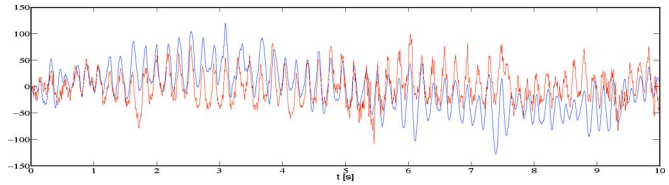


Fig. 15. (Blue) Extracted seizure activity plotted against (red) 20th channel of the EEG recording. It is clear that the extracted activity is in phase with the activity from channel 20.

immediately after the muscle activity, when the muscle is still not in the completely relaxed state. However, the muscle is not in complete rest, and therefore, the power of the EMG signal is still fairly high. This is a very useful application of our algorithm, because otherwise the EMG activity here cannot be accurately studied. In the middle trace of Fig. 16, the extracted ECG artifact is shown, and the lower trace shows the cleaned EMG signal obtained by subtracting the extracted artifact from the original signal.

B. Results and Discussion

We showed results of applying our technique to real-life examples. In Fig. 14, the T1 channel of the EEG recordings is decomposed. After applying the EEMD–ICA algorithm, seven ICs were extracted among which we show three to back reconstruct the signals shown in Fig. 14, representing the seizure event, eye artifact, and muscle activity, respectively. We can clearly note a successful separation of the important components. The extracted oscillatory activity is in phase with the seizure activity visible in the T2 channel (see Fig. 15). This confirms that this is related to the seizure. This is an interesting result, since channels T1 and T2 are located on the opposite sides of the head. This means that the seizure has been picked up from the averaged reference despite the very low SNR. It is also clear that the eye artifact is more clearly (although not perfectly) expressed than in the original signal and that the muscle activity is well separated. We would like to stress here that these artifacts (e.g., eye artifact) can sometimes be more clear in other leads (Fp1 and Fp2). However, in some cases (e.g., in neonates), EEG is recorded only with eight, and sometimes even with as few as two leads. In these cases, it is very difficult to capture all the brain activity clearly, and our algorithm can be beneficial.

Fig. 16 shows the EMG signal contaminated by the ECG artifact. In the middle trace of Fig. 16, the extracted ECG artifact is shown, and the lower trace shows the cleaned EMG signal

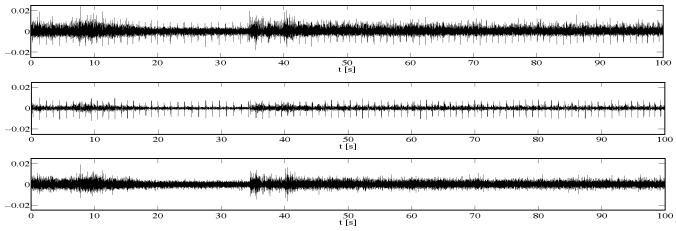


Fig. 16. EMG recording. Upper trace—original EMG signal, middle trace—extracted ECG artifact, and lower trace—cleaned EMG signal. np was set to 0.5.

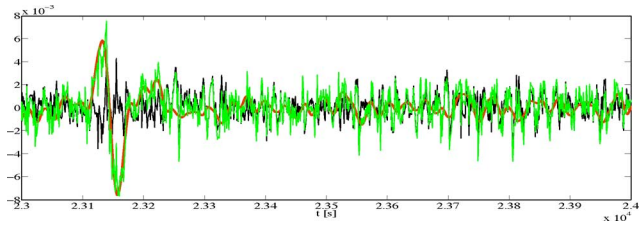


Fig. 17. Enhanced part of the real-life EMG signal is shown, contaminated by the (green) ECG artifact, (red) extracted ECG artifact, and (black) cleaned EMG signal.

obtained by subtracting the extracted artifact from the original signal. We see that the ECG artifact is nicely removed from the signal without distorting the original shape and amplitude of the EMG signal. After applying the EEMD–ICA algorithm, four sources were detected, only one of them containing the ECG artifact. As one can think that some EMG activity is also mixed into the ECG source, Fig. 17 zooms in a 1 s of the signal from Fig. 16 to show the performance of the proposed algorithm in detail. In Fig. 17, the extracted artifact and the clean version of the EMG are shown. It is clear that the spike is nicely isolated (red trace), and the cleaned EMG closely follows local variations of the original EMG in the places where the spike is not present. The channel in which the spike appears still contains some small oscillations that are not spike-related. However, these oscillations are very slow and small in amplitude, so they do not significantly change the shape of the EMG signal, and therefore will not influence various measures of the EMG activity derived afterward. The computed ratio of the SD of the cleaned EMG signal to the SD of the ECG artifact is 1, which is fairly high. The np in these applications was set to 0.5.

V. Conclusion

A new method for single-channel signal decomposition into its ICs, which combines EEMD [10], [19] and ICA, EEMD–ICA has been presented. We showed the good performance of the method and compared it to two other available algorithms for decomposing single-channel signals, WICA [11] and SCICA [9] through various simulations. Of the three algorithms, SCICA had the worst performance. The WICA technique, although comparable with the EEMD–ICA, shows a weaker performance in our simulations. We provided the two real-life examples and our technique exhibited a very strong separation power, and proved to be successful for oscillatory as well as spike-type source extraction in biomedical signal processing.

REFERENCES

[1] T. Jung, S. Makeig, C. Humphries, T. Lee, M. McKeown, V. Iragui, and T. Sejnowski, "Removing electroencephalographic artifacts by blind source separation," *Psychophysiology*, vol. 37, pp. 163–178, 2000.

[2] V. Calhoun, J. Liu, and T. Adali, "A review of group ICA for fMRI data and ICA for joint inference of imaging, genetic, and ERP data," *Neuroimage*, vol. 45, no. 1, pp. 163–172, 2009.

[3] M. De Vos, A. Vergult, L. De Lathauwer, W. De Clercq, S. Van Huffel, P. Dupont, A. Palmini, and W. Van Paesschen, "Canonical decomposition of ictal scalp EEG reliably detects the seizure onset zone," *NeuroImage*, vol. 37, no. 3, pp. 844–854, 2007.

[4] L. De Lathauwer, J. Castaing, and J.-F. Cardoso, "Fourth-order cumulant based underdetermined independent component analysis," *IEEE Trans. Signal Process.*, vol. 55, no. 6, pp. 2965–2973, Feb. 2007.

[5] P. Zhou and T. Kuiken, "Eliminating cardiac contamination from myoelectric control signals developed by targeted muscle reinnervation," *Physiol. Meas.*, vol. 27, pp. 1311–1327, 2006.

[6] J. Taelman, A. Spaepen, and S. Van Huffel, "Wavelet-independent component analysis to remove electrocardiography contamination in surface electromyography," in *Proc. Eng. Med. Biol. Soc.*, 2007, pp. 682–685.

[7] U. Rutishauser, E. M. Schuman, and A. N. Mamelak, "Online detection and sorting of extracellularly recorded action potentials in human medial temporal lobe recordings, in vivo," *J. Neurosci. Methods*, vol. 154, pp. 204–224, 2006.

[8] M. Lewicki, "A review of methods for spike sorting: The detection and classification of neural action potentials," *Comput. Neural Syst.*, vol. 9, no. 4, pp. R53–R78, 1998.

[9] M. E. Davies and C. J. James, "Source separation using single channel ICA," *Signal Process.*, vol. 87, no. 8, pp. 1819–1832, 2007.

[10] N. E. Huang, M. L. Wu, S. R. Long, S. S. Shen, W. D. Qu, P. Gloersen, and K. L. Fan, "The empirical mode decomposition and the hilbert spectrum for nonlinear and non-stationary time series analysis," *Proc. Royal Soc. London*, vol. 454A, no. 1971, pp. 903–993, 1998.

[11] J. Lin and A. Zhang, "Fault feature separation using wavelet-ICA filter," *NDT & E Int.*, vol. 38, no. 6, pp. 421–427, 2005.

[12] B. Azzerboni, G. Finocchio, M. Ipsale, F. L. Foresta, and F. Morabito, "A new approach to detection of muscle activation by independent component analysis and wavelet transform," in *Lecture Notes in Computer Sciences*, vol. 2486. Heidelberg, Germany: Springer-Verlag, Sep. 2002, pp. 109–116.

[13] B. Azzerboni, F. L. Foresta, N. Mammone, and F. Morabito, "A new approach based on wavelet-ICA algorithms for fetal electrocardiogram extraction," in *Proc. Eur. Symp. Artif. Neural Netw. (ESANN)*, Bruges, Apr. 2005, pp. 193–198.

[14] P. Flandrin and P. Goncalves, "Empirical mode decomposition as data-driven wavelet-like expansion," *Int. J. Wavel., Multires. Inf. Proc.*, vol. 2, no. 4, pp. 477–496, 2004.

[15] H. Xing and J. Hou, "Electrocardiogram noise removal based on empirical mode decomposition and independent component analysis," *J. Clin. Rehabil. Tissue Eng. Res.*, vol. 13, no. 4, pp. 652–654, 2009.

[16] A. Hyvarinen and E. Oja, "Independent component analysis: Algorithms and applications," *Neural Netw.*, vol. 13, no. 4/5, pp. 411–430, 2000.

[17] Fastica Graphical User Interface. (2005). [Online]. Available: http://www.cis.hut.fi/projects/ica/fastica/code/dlcode.shtml

[18] I. Daubechies, E. Roussos, S. Takerkart, M. Benharrosh, C. Golden, K. D'Ardenne, W. Richter, J. D. Cohen, and J. Haxby, "Independent component analysis for brain fMRI does not select for independence," *Proc. Nat. Acad. Sci. USA*, vol. 106, no. 42, pp. 10 415–10 422, 2009.

[19] Z. Wu and N. E. Huang, "Ensemble empirical mode decomposition: A noise-assisted data analysis method," *Adv. Adaptive Data Anal.*, vol. 1, no. 1, pp. 1–41, 2009.

[20] Ensembleemd Algorithm. (2008). [Online]. Available: http://rcada.ncu.edu.tw/research1_clip_program.html

[21] W. Deburchgraeve, P. J. Cherian, M. De Vos, R. M. Swarte, J. H. Blok, G. H. Visser, P. Govaert, and S. Van Huffel, "Automated neonatal seizure detection mimicking a human observer reading EEG," *Clin. Neurophysiol.*, vol. 119, no. 11, pp. 2447–2454, 2008.

[22] A. Bell and T. Sejnowski, "An information-maximization approach to blind separation and blind deconvolution," *Neural Comput.*, vol. 7, no. 6, pp. 1129–1159, 1995.

[23] J. Cardoso and A. Souloumiac, "Blind beamforming for non gaussian signals," *Inst. Electr. Eng. F—Radar Signal Process.*, vol. 140, no. 6, pp. 362–370, 1993.



Bogdan Mijović (S'08) was born in Belgrade, Serbia. He received the M.Sc. degree in electrical engineering from the University of Belgrade, Belgrade, Serbia, in May 2007. Since March 208, he has been working toward the Graduate degree in the Biomed group, Department of Electrical Engineering, SCD Division, Katholieke Universiteit Leuven, Leuven, Belgium.

His current research interests include development of single and multichannel signal-processing algorithms and their applications in biomonitoring, including multimodal integration of different physiological signals.



Maarten De Vos (M'09) was born in Duffel, Belgium, in 1983. He received the M.Sc. degree in electrotechnical-mechanical engineering, with specialization in biomedical techniques, and the Ph.D. degree in engineering from the Katholieke Universiteit Leuven (K. U. Leuven), Leuven, Belgium, in 2005 and 2009, respectively.

Since 2009, he has been a Postdoctoral Researcher in the Electrical Engineering Department, SCD Division, K. U. Leuven. His current research interests include linear and multilinear algebra and decomposition techniques for biomedical signals.



Ivan Gligorijević received the M.Sc. degree in electrical engineering from the University of Belgrade, Belgrade, Serbia, in July 2008. Since January 2009, he has been working toward the Ph.D. degree in the Biomed group, Department of Electrical Engineering, SCD Division, Katholieke Universiteit Leuven, Leuven, Belgium.

His current research interests include developing signal-processing solutions for closing the loop between deep brain stimulation and recording for microarray probes in cooperation with IMEC, Belgium.



Joachim Taelman (M'08) was born in Roeselare, Belgium, in 1982. He received the M.Sc. degree in electrotechnical-mechanical engineering, with specialization in biomedical technique, from the Department of Electrical Engineering, Katholieke Universiteit Leuven, Leuven, Belgium, in June 2006, where he is currently working toward the Ph.D. degree.

His current research interests include biomedical signal processing and special interest in electromyogram and electrocardiogram analysis for several applications.



Sabine Van Huffel (M'96–A'96–SM'99–F'09) received the M.D. degree in computer science engineering, the M.D. degree in biomedical engineering, and the Ph.D. degree in electrical engineering from Katholieke Universiteit Leuven (K. U. Leuven), Leuven, Belgium, in June 1981, July 1985, and June 1987, respectively.

She is currently a Full Professor in the Department of Electrical Engineering, K. U. Leuven. Her research interests include numerical (multi)linear algebra and software, system identification, parameter estimation, and biomedical data processing.